Acta Crystallographica Section F
Structural Biology and Crystallization Communications
ISSN 1744-3091

Purification, crystallization and preliminary X-ray crystallographic analysis of the transport unit of the monomeric autotransporter AIDA-I from *Escherichia coli*

Iris Gawarzewski,[a] Britta Tschapek,[a] Astrid Hoeppner,[b] Joachim Jose,[c] Sander H. J. Smits[a] and Lutz Schmitt[a]*

[a]Institute of Biochemistry, Heinrich-Heine-Universität, Düsseldorf, Germany, [b]Crystal Farm and X-ray Facility, Heinrich-Heine-Universität, Düsseldorf, Germany, and [c]Institute of Pharmaceutical and Medical Chemistry, Westfälische Wilhems-Universität, Münster, Germany

Correspondence e-mail: lutz.schmitt@hhu.de

Received 4 July 2013
Accepted 1 September 2013

The adhesin involved in diffuse adherence (AIDA-I) from *Escherichia coli* belongs to the group of autotransporters, specifically the type Va secretion system (T5aSS). All autotransporter systems contain a C-terminal β-domain, which forms a barrel-like structure in the outer membrane with a hydrophilic pore allowing passenger translocation across the outer membrane. The passenger domain harbours the biological activity in the extracellular space and functions, for example, as an adhesin, an enzyme and a toxin. The exact transport mechanism of passenger translocation across the outer membrane is not clear at present. Thus, structure determination of the transport unit of AIDA-I could provide new insights into the transport mechanism. Here, the purification, crystallization and preliminary X-ray crystallographic studies of the transport unit of AIDA-I are reported.

1. Introduction

Benz & Schmidt (1989) described the adhesin involved in diffuse adherence glycoprotein I (AIDA-I) of enteropathogenic *Escherichia coli* (EPEC), which was found in a patient suffering from infantile diarrhoea. Several studies revealed that AIDA-I is transported in a similar way to the IgA protease from *Neisseria gonorrhoea*, the prototype of monomeric autotransporter proteins (Pohlner *et al.*, 1987; Henderson *et al.*, 2004; Jose & Meyer, 2007). Subsequently, AIDA-I was assigned to the group of monomeric autotransporters (subgroup Va; Leo *et al.*, 2012).

In general, monomeric autotransporters consist of four functional domains encoded in one polypeptide chain: (i) an N-terminal signal peptide mediating transport across the inner membrane *via* the Sec translocon; (ii) a passenger domain harbouring the biological functionality in the extracellular space; (iii) a linker domain connecting the passenger domain and the β-domain; and (iv) a β-domain forming a β-barrel-like structure in the outer membrane at the C-terminus (Jose, 2006). Despite numerous studies on the autotransporter secretion pathway, the exact translocation process of the passenger domain across the outer membrane remains largely unknown. Different transport models have been proposed to try to explain recent results, *i.e.* the hairpin model and the Omp85 model (Bernstein, 2007; Shahid *et al.*, 2012). Recently, a new model mechanism was described which is a combination of both the hairpin model and the Omp85 model (Ieva *et al.*, 2011; Pavlova *et al.*, 2013). To gain further insights into this process, we crystallized the recombinant transport unit of AIDA-I for structure determination by X-ray diffraction. Here, we describe the preliminary results of the expression, purification and crystallization of the transport unit of AIDA-I from *E. coli*.

2. Materials and methods

2.1. Cloning, expression and membrane preparation

The recombinant autotransporter protein used in this study consisted of an N-terminal His_6 tag, an epitope for immunodetection

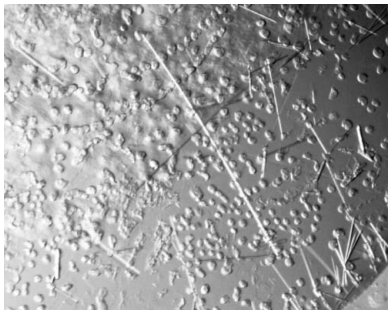

as a passenger domain, the AIDA-I linker domain comprising 163 amino acids and the AIDA-I β-domain (see §2.1 of the Supplementary Material[1]). Thus, this fusion protein was termed FP-HisN163 with a theoretical molecular weight of 50.9 kDa. The gene encoding FP-HisN163 was cloned into the expression vector pJM007 (Maurer *et al.*, 1997), resulting in plasmid pIG501. The constitutive expression of FP-HisN163 was performed in 12 l cell culture with *E. coli* UT5600 (DE3) for 18 h at 303 K and 170 rev min^{-1} to a final OD_{600} of 4.4. Cells were harvested at 277 K and 7000*g* for 10 min. All subsequent steps were conducted at 277 K. Cell pellets were resuspended in 200 ml of 200 m*M* Tris–HCl pH 8.0, 200 m*M* NaCl, 0.1 mg ml^{-1} DNase and were disrupted by several passes through a cell disrupter at 2.5 MPa (Constant Systems). Non-disrupted cells and cell debris were removed by a centrifugation step at 19 000*g* for 45 min. Using the supernatant, membrane fractions were isolated by ultracentrifugation at 200 000*g* for 1 h 15 min, homogenized in 200 m*M* Tris–HCl, 200 m*M* NaCl, 10% glycerol and diluted to a final concentration of 100 mg ml^{-1}.

2.2. Detergent screen

For solubilization of FP-HisN163, aliquots of membrane fractions were mixed with a final concentration of 1%(*v*/*v*) of each tested detergent (see §2.2 of the Supplementary Material) and incubated at 310 K and 800 rev min^{-1} for 1 h. After ultracentrifugation at 200 000*g* and 277 K for 30 min, pellet and supernatant fractions were applied to western blotting analysis using an anti-His antibody for subsequent immunodetection.

2.3. Purification

The membrane fractions were solubilized with 1%(*v*/*v*) *N*,*N*-dimethyldodecylamine *N*-oxide (LDAO) for 1 h at 310 K and 70 rev min^{-1} followed by an ultracentrifugation step at 200 000*g* and 277 K for 30 min. All subsequent purification steps were performed at 277 K. The supernatant was first applied onto an immobilized metal-ion affinity chromatography (IMAC) column (data not shown). The collected fractions were analyzed by SDS–PAGE and concentrated with an Amicon Ultra Centrifugal Filter device (30 kDa molecular-weight cutoff, Millipore) to a final concentration of 4 mg ml^{-1}. In the second purification step size-exclusion chromatography (SEC) with a Superdex 200 10/30 column (GE Healthcare) was performed with 20 m*M* HEPES pH 7.5, 150 m*M* NaCl, 2.8 m*M* LDAO (data not shown). Fractions were collected, analyzed by SDS–PAGE and concentrated with an Amicon Ultra Centrifugal Filter device (30 kDa molecular-weight cutoff, Millipore) to achieve final concentrations between 7 and 28 mg ml^{-1}. The purification procedure yielded 2 mg pure protein from 12 l culture. Protein concentration was determined with a NanoDrop device (PeqLab Biotechnology GmbH) using the molecular mass of FP-HisN163 (50.90 kDa including the His_6 tag) and its calculated extinction coefficient (84.80 M^{-1} cm^{-1}; http://web.expasy.org/protparam).

2.4. Denaturation analysis

The purified protein samples of FP-HisN163 were prepared for SDS–PAGE analysis with sample buffers *A* [3.2%(*w*/*v*) SDS] and *B* [6.4%(*w*/*v*) SDS]. These samples were heated at 373 K for 0, 5, 10, 15, 20, 25 and 30 min, respectively.

[1] Supplementary material has been deposited in the IUCr electronic archive (Reference: WD5224).

2.5. Crystallization and preliminary X-ray analysis

Initial screening for crystallization conditions was performed at 291 K using the hanging-drop vapour-diffusion method combined with commercially available buffer screens (MemPlus from Molecular Dimensions and JCSG Suites I–IV from Qiagen). Needle-like crystals were observed after 2–3 weeks by mixing equal volumes of protein and precipitant solution. The primary crystallization condition [100 m*M* sodium cacodylate pH 6.5, 12.5%(*v*/*v*) PEG 2000 MME] was optimized to a final condition consisting of 100 m*M* sodium cacodylate pH 6.5, 27.5%(*v*/*v*) PEG 2000 MME, resulting in rod-like crystals with maximum dimensions of 20 × 20 × 200 µm. Crystals were soaked in cryoprotective buffer [the crystallization condition plus an additional 10%(*v*/*v*) PEG 2000 MME and 10 m*M* LDAO] and flash-cooled in liquid nitrogen. A data set was collected from a single crystal on ESRF beamline ID23-eh2. The data set was processed using the *XDS* package (Kabsch, 2010*b*) and scaled with *XSCALE* (Kabsch, 2010*a*).

3. Results

The recombinant autotransporter protein FP-HisN163 carrying the transport unit of the monomeric autotransporter AIDA-I was expressed in *E. coli* UT5600 (DE3). Since FP-HisN163 is embedded in the outer membrane a suitable detergent had to be found for solubilization, for which a screen was performed using membrane fractions and different detergents at a final concentration of 1%(*v*/*v*) (see §2.2). Of all of the detergents tested, LDAO showed the highest solubilization efficiency. LDAO is likewise the detergent that was used for the solubilization and crystallization of other membrane proteins (Camara-Artigas *et al.*, 2002; Yue *et al.*, 2003; van den Berg *et al.*, 2004). Thus, LDAO was used in all subsequent purification steps. FP-HisN163 was first isolated using IMAC (see §2.3; data not shown). As a second purification step SEC was performed with the concentrated fractions of the elution peak resulting from IMAC (see §2.3; data not shown). The pooled fractions were concentrated to a final concentration of between 7 and 28 mg ml^{-1}.

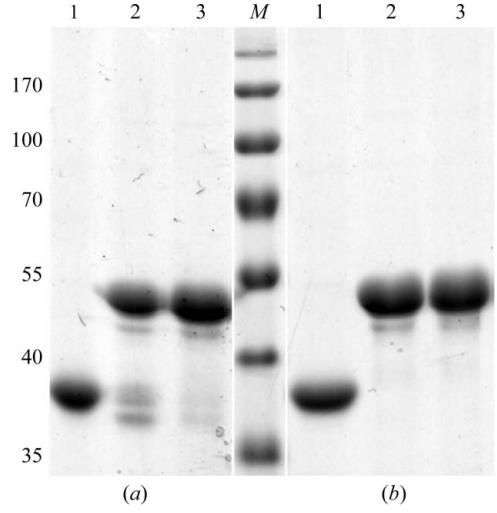

Figure 1
Denaturation analysis of purified FP-HisN163 by Coomassie-stained SDS–PAGE. (*a*) SDS sample buffer with 3.2%(*w*/*v*) SDS (lanes 1–3). (*b*) SDS sample buffer with 6.4%(*w*/*v*) SDS (lanes 1–3). Lane *M*, PageRuler Prestained Protein Ladder (Fermentas; labelled in kDa on the left); lane 1, not heated; lane 2, heated for 5 min; lane 3, heated for 10 min. The samples were heated to 373 K.

Table 1
Data-collection statistics.

Values in parentheses are for the outermost resolution shell.

No. of crystals	1
Beamline	ID23-eh2, ESRF
Temperature (K)	100
Wavelength (Å)	0.8726
Detector	MAR Mosaic 225 mm
Crystal-to-detector distance (mm)	375.71
Rotation range per image (°)	1.35
Total rotation range (°)	108
Exposure time per image (s)	2.168
Resolution range (Å)	50–3.15 (3.20–3.15)
Space group	$P2_12_12$ or $P2_12_12_1$
Unit-cell parameters	
a (Å)	40.33
b (Å)	85.85
c (Å)	134.05
$\alpha = \beta = \gamma$ (°)	90
Mosaicity (°)	0.78
Total No. of measured intensities	36648 (1606)
Unique reflections	7899 (348)
Multiplicity	4.64 (4.61)
Completeness (%)	92.3 (94.3)
$R_{\rm meas}$† (%)	9.5 (49.7)
$R_{\rm p.i.m.}$‡ (%)	4.0 (18.2)
$\langle I/\sigma(I)\rangle$	15.38 (3.34)
Overall B factor from Wilson plot (Å^2)	48.29

† $R_{\rm meas} = \sum_{hkl}\{N(hkl)/[N(hkl)-1]\}^{1/2}\sum_i |I_i(hkl) - \langle I(hkl)\rangle|/\sum_{hkl}\sum_i I_i(hkl)$. ‡ $R_{\rm p.i.m.} = \sum_{hkl}\{1/[N(hkl)-1]\}^{1/2}\sum_i |I_i(hkl) - \langle I(hkl)\rangle|/\sum_{hkl}\sum_i I_i(hkl)$.

It is known that outer membrane proteins are very stable at room temperature even upon addition of SDS and show abnormal migration behaviour during SDS–PAGE analysis owing to their compact folding (de Cock *et al.*, 1996; Sugawara *et al.*, 1996; Maurer *et al.*, 1999). When analyzing the sample by SDS–PAGE, FP-HisN163 migrates at a lower molecular mass than expected (Fig. 1). The different sample buffers *A* and *B* were added to aliquots of purified FP-HisN163 and then heated at 373 K for different time periods (see §2.4). The non-heated protein was detected at a molecular weight of 39 kDa independently of the applied sample buffer (Fig. 1, lane 1). After 5 min of heating at 373 K in sample buffer *A* three bands were observed at molecular weights of 50, 39 and 37 kDa (Fig. 1*a*, lane 2). The protein bands at 37 and 39 kDa disappeared with increased heating time in sample buffer *A* and were identified as denaturation artifacts. These protein bands were not detected using sample buffer *B* even at the shortest heating time (Fig. 1*b*, lane 2). Therefore, for all other samples and SDS–PAGE analysis buffer *B* and a short heating procedure were used.

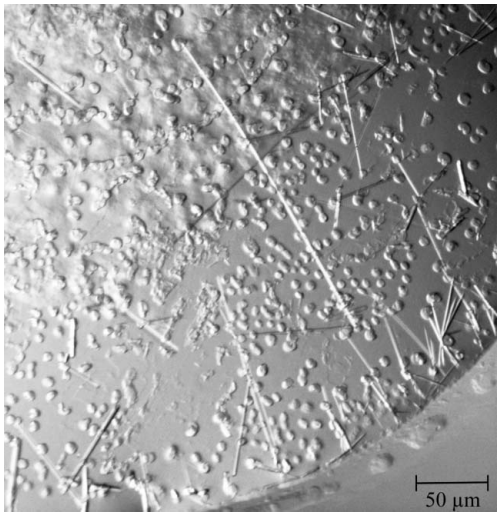

Figure 2
Needle crystals of FP-HisN163 with dimensions of 20 × 20 × 200 µm.

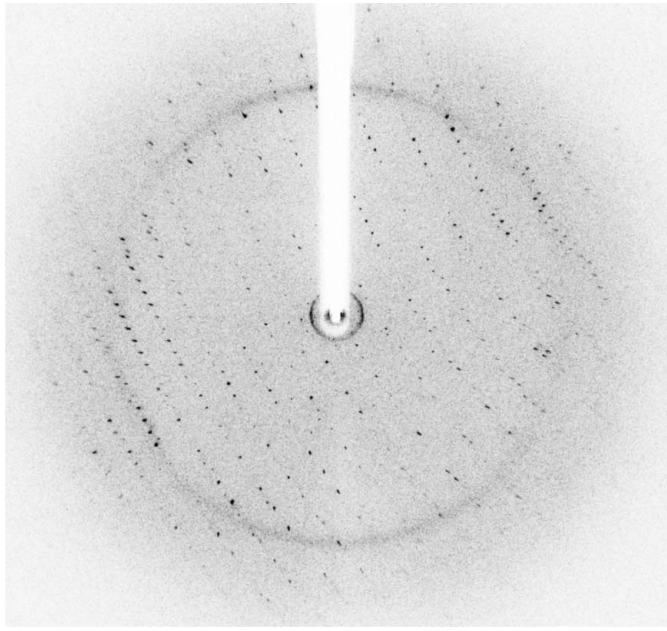

Figure 3
Diffraction image collected with a rotation width of 1.35°.

Crystals grew in various crystallization conditions using the hanging-drop vapour-diffusion method (see §2.5). Well diffracting crystals were obtained after 40 d at 291 K in 100 m*M* sodium cacodylate pH 6.5, 27.5%(*v*/*v*) PEG 2000 MME (Fig. 2). Crystals were transferred into cryobuffer, flash-cooled and a native data set was collected. The crystals diffracted to a resolution of 3.15 Å (Table 1; Fig. 3).

Preliminary processing of the data set using the *XDS* package and self-rotation analysis using the data processed in *P*1 revealed that the crystals belonged to a primitive orthorhombic space group with unit-cell parameters a = 40.33, b = 85.85, c = 134.05 Å. At present we cannot distinguish between space group $P2_12_12$ and $P2_12_12_1$, since the systematic absences observed are not conclusive (see Table 1 for data statistics). The unit-cell content analysis suggests the presence of one monomer (50.10 kDa) in the asymmetric unit with a $V_{\rm M}$ value of 2.32 Å^3 Da^{-1} and a solvent content of 47%(*v*/*v*) (Matthews, 1968). Structure determination is currently in progress.

We thank the staff of ESRF beamline ID23-eh2 and the EMBL Hamburg staff for support and assistance during crystal screening and data collection. We also gratefully acknowledge support (and training) from the International NRW Research School BioStruct granted by the Ministry of Innovation, Science and Research of the State North Rhine-Westphalia, Heinrich-Heine-University Düsseldorf and the Entrepreneur Foundation at Heinrich-Heine-University Düsseldorf.

References

Benz, I. & Schmidt, M. A. (1989). *Infect. Immun.* **57**, 1506–1511.
Berg, B. van den, Black, P. N., Clemons, W. M. Jr & Rapoport, T. A. (2004). *Science*, **304**, 1506–1509.
Bernstein, H. D. (2007). *Trends Microbiol.* **15**, 441–447.
Camara-Artigas, A., Brune, D. & Allen, J. P. (2002). *Proc. Natl Acad. Sci. USA*, **99**, 11055–11060.

Cock, H. de, van Blokland, S. & Tommassen, J. (1996). *J. Biol. Chem.* **271**, 12885–12890.
Henderson, I. R., Navarro-Garcia, F., Desvaux, M., Fernandez, R. C. & Ala'Aldeen, D. (2004). *Microbiol. Mol. Biol. Rev.* **68**, 692–744.
Ieva, R., Tian, P., Peterson, J. H. & Bernstein, H. D. (2011). *Proc. Natl Acad. Sci. USA*, **108**, E383–E391.
Jose, J. (2006). *Appl. Microbiol. Biotechnol.* **69**, 607–614.
Jose, J. & Meyer, T. F. (2007). *Microbiol. Mol. Biol. Rev.* **71**, 600–619.
Kabsch, W. (2010*a*). *Acta Cryst.* D**66**, 133–144.
Kabsch, W. (2010*b*). *Acta Cryst.* D**66**, 125–132.
Leo, J. C., Grin, I. & Linke, D. (2012). *Philos. Trans. R. Soc. Lond. B Biol. Sci.* **367**, 1088–1101.
Matthews, B. W. (1968). *J. Mol. Biol.* **33**, 491–497.
Maurer, J., Jose, J. & Meyer, T. F. (1997). *J. Bacteriol.* **179**, 794–804.
Maurer, J., Jose, J. & Meyer, T. F. (1999). *J. Bacteriol.* **181**, 7014–7020.
Pavlova, O., Peterson, J. H., Ieva, R. & Bernstein, H. D. (2013). *Proc. Natl Acad. Sci. USA*, **110**, E938–E947.
Pohlner, J., Halter, R., Beyreuther, K. & Meyer, T. F. (1987). *Nature (London)*, **325**, 458–462.
Shahid, S. A., Bardiaux, B., Franks, W. T., Krabben, L., Habeck, M., van Rossum, B. J. & Linke, D. (2012). *Nature Methods*, **9**, 1212–1217.
Sugawara, E., Steiert, M., Rouhani, S. & Nikaido, H. (1996). *J. Bacteriol.* **178**, 6067–6069.
Yue, W. W., Grizot, S. & Buchanan, S. K. (2003). *J. Mol. Biol.* **332**, 353–368.